Mounds in Oxia Planum: The Burial and Exhumation of the ExoMars Rover Landing Site

Journal Item

Mounds in Oxia Planum: The Burial and Exhumation of the ExoMars Rover Landing Site

Joseph D. McNeil[1*], Peter Fawdon[1], Matthew R. Balme[1], Angela L. Coe[2], Nicolas Thomas[3]

[1]School of Physical Sciences, The Open University, Walton Hall, Milton Keynes, MK7 6AA, UK

[2]School of Earth, Environment and Ecosystem Sciences, The Open University, Walton Hall, Milton Keynes, MK7 6AA, UK

[3]Physikalisches Institut, University of Bern, Sidlerstrasse. 5, 3012, Bern, Switzerland

*Corresponding author: Joseph D. McNeil (joe.mcneil@open.ac.uk)

Key Points:

- Mounds in Oxia Planum represent eroded remnants of a circum-Chryse deposit that was up to 130 m thick in the ExoMars rover landing site.
- The mounds unconformably overlie the clay-bearing unit and are in turn unconformably onlapped by the dark resistant unit.
- The plains immediately adjacent to the mounds are the most recently exposed parts of the astrobiologically important clay-bearing unit.

This article has been accepted for publication and undergone full peer review but has not been through the copyediting, typesetting, pagination and proofreading process, which may lead to differences between this version and the Version of Record. Please cite this article as doi: 10.1029/2022JE007246.

Abstract

Oxia Planum, the planned landing site of the ExoMars '*Rosalind Franklin*' rover, is a low relief clay-bearing plain, of which approximately 1% is covered by 396 upstanding isolated landforms ('mounds'). The mounds are continuous with a circum-Chryse mound population representing the remnants of a regionally significant Noachian-aged deposit. This detailed study suggests that the Oxia Planum mounds are also erosional remnants of this deposit, with little evidence to suggest they are constructional landforms such as sedimentary volcanoes. We calculate that up to 130 meters of mound-forming material has been removed from the landing site through erosion. The mound-forming layer lies unconformably on the clay-bearing plains with the upper surface severely truncated by significant erosion resulting in the topography we see today. The mounds themselves comprise at least three members, distinct in color and texture, separated stratigraphically by further unconformities. Calculated minimum erosion/deposition rates of the removed mound material are comparable to previous Noachian estimates, suggesting a more erosive (and probably therefore warmer and/or wetter) environment than today. The clay-bearing materials which remain buried directly under the mounds have been continually protected from the martian environment since the Noachian, and are likely to represent some of the most pristine clay-rich materials in the landing site. By inference, the plains directly adjacent to the mounds are most likely to have been exposed for less time than areas further from the mounds. These are therefore amongst the most likely locations where *Rosalind Franklin* could sample recently exposed materials and hence detect biosignatures.

Plain Language Summary

The Oxia Planum region of Mars is the landing site of ESA's ExoMars '*Rosalind Franklin*' rover, which will search for evidence of past life in the ancient rocks of the area. In the landing site there are hundreds of sub-kilometer-scale "mounds" that are likely to have been part of an extensive layer which covered the region in the distant past. To understand more about the mounds, we examined their geological features, calculated the volume of eroded material, and observed their relationships to other important features within the landing site. We find: (1) On average, the layer was up to 70% thinner in Oxia Planum than elsewhere in the region. (2) There are gaps in the geological record below, within, and above the mounds indicating periods of erosion. (3) The layer was eroded at a much faster rate in the past than in the present, consistent with a warmer and wetter

ancient martian environment. Areas around the mounds were probably exposed relatively recently, and are therefore likely to have been protected from the harsh martian environment for longer than other areas. Consequently, these areas may be amongst the best places for the rover to search for evidence of past life.

1 Introduction

Oxia Planum is the planned landing site of ESA's ExoMars '*Rosalind Franklin'* rover (Vago et al., 2017). This low-relief plain is situated on the hemispheric dichotomy boundary in the transitional terrain (classified as HNCc1 - Early Hesperian to Late Noachian in Tanaka et al., (2005)) between the ancient, rugged highlands of Arabia Terra and the younger, smoother lowlands of Chryse Planitia. *Rosalind Franklin* will investigate the surface and subsurface geologic and geochemical environments of Oxia Planum, with a primary objective to search for evidence of extinct life through the identification of potential habitable paleoenvironments and biosignatures (Vago et al., 2017). Oxia Planum contains a diversity of Noachian-aged geologic features and geochemical characteristics which make it a suitable candidate for astrobiological exploration, including extensive Fe/Mg-rich clay-bearing plains indicative of widespread aqueous alteration (e.g. Parkes Bowen et al., 2022; Brossier et al., 2022; Carter et al., 2016; Gary-Bicas & Rogers, 2021; Mandon et al., 2021; Quantin-Nataf et al., 2021), a hydrated silica-bearing sedimentary fan at the terminus of the Coogoon Valles network suggesting the presence of a standing body of water (e.g. Fawdon et al., 2021a; Quantin-Nataf et al., 2021; Molina et al., 2017), and a series of landforms revealing a complex depositional and erosional history (Quantin-Nataf et al., 2021; Roberts et al., 2021).

The widely exposed clay-bearing plains will be the focus of *Rosalind Franklin's* biosignature detection and surface/subsurface aqueous environment investigations. The clay-bearing plains are bright-toned, highly fractured, low-relief regions that are consistent with detections of phyllosilicates by OMEGA (Observatoire pour la Minéralogie, l'Eau, les Glaces et l'Activité; Bibring et al., 2004) and absorption spectra in hyperspectral CRISM (Compact Reconnaissance Imaging Spectrometer for Mars; Murchie et al., 2007) data which correspond to Fe/Mg-rich phyllosilicates such as vermiculite and/or smectite clays (Parkes Bowen et al., 2022; Mandon et al., 2021; Carter et al., 2016). The clay-bearing plains contain at least two distinct geologic members (Mandon et al., 2021). These are a lower, thicker member which exhibits orange tones in HiRISE (High Resolution Imaging Science Experiment; McEwen et al., 2007) images and contains closely spaced meter-scale fractures, and overlying this, an upper, thinner member which exhibits blue-white tones in HiRISE and contains more widely spaced decameter-scale fractures (Parkes Bowen et al., 2022; Quantin-Nataf et al., 2021).

Overlying the clay-bearing plains is a population of kilometer to sub-kilometer-scale mounds (Figure 1), which resemble terrestrial erosional features such as buttes (e.g. Monument Valley, Utah/Arizona), mesas (e.g. Grand Mesa, Colorado), inselbergs (e.g. Uluru, Australia), and hills (McNeil et al., 2021; Quantin-Nataf et al., 2021). These mounds are topographically prominent features which represent three-dimensional exposures of material accessible for study by *Rosalind Franklin*. Their relatively high albedo in CTX (Context Camera; Malin et al., 2007) and white-yellow tones in CaSSIS (Colour and Stereo Surface Imaging System; Thomas et al., 2017) NPB products (Near-IR, Panchromatic, Blue-Green, see section 2) contrast with the orange-blue tones of the surrounding clay-bearing plains in HiRISE and CaSSIS (Parkes Bowen et al., 2022; Quantin-Nataf et al., 2021).

The mounds are part of a regional population of similar positive-relief isolated landforms that occur around the highland margin of Chryse Planitia (Figure 1a). This wider population of over 14,000 kilometer-scale mounds is interpreted as the eroded remnants of a layer, up to 500 m thick, that superposed the circum-Chryse region during the Noachian and may be similar in age and composition to the Mawrth Vallis phyllosilicates (McNeil et al., 2021). Prior to this study, it was unclear how the smaller Oxia Planum mounds relate to the circum-Chryse layer-forming population. The smaller size of the mounds in Oxia Planum means that a higher resolution examination is required to understand their geology, and to determine whether these are landforms which are part of the original circum-Chryse mound-forming layer (and are therefore erosional in nature), or whether they are individual landforms formed through geographically isolated processes (and are therefore primarily constructional). The mounds in Oxia Planum overlie the clay-bearing plains (McNeil et al., 2021; Quantin-Nataf et al., 2021), and could therefore record depositional processes which occurred after the deposition or emplacement of the plains. Furthermore, because the mounds could be erosional remnants, they may provide information about subsequent erosional processes in Oxia Planum. Previous models have suggested that up to 900 m of material has been removed from the landing site (Quantin-Nataf et al., 2021), but how much belonged to individual mounds or the hypothetical mound-forming layer compared to the clay-bearing plains or other stratigraphic units at the landing site, is unknown.

In this paper, we: (1) Explore the morphology, morphometry, and stratigraphic relationships of mounds in Oxia Planum; (2) Assess whether the mounds originated as constructional landforms in their current isolated locations, or if they are erosional features which were once part of previously more laterally extensive deposits; and (3) Calculate the hypothetical thickness and volume of the putative mound-forming layer to assess the quantity and timing of overburden removal from the landing site and the feasibility of this hypothesis. From this, we discuss the implications for the geology of the mounds, the depositional and erosional history of the landing site, and the ramifications for the scientific objectives of the '*Rosalind Franklin'* rover.

2 Data and Methods

We have used the informal geographical names given to features and regions of the landing site by the ExoMars *Rosalind Franklin* rover team (see Fawdon et al., 2021b). Using ArcGIS Pro software, we created a Geographical Information Systems (GIS) project for the study area and included all available remote sensing data. Mounds (upstanding, bright-toned, topographically prominent features) were identified using a combination of visible (CaSSIS, HiRISE and CTX) and topographic (CTX and HiRISE) data in the ~8700 km^2 study area (Figure 1). Geologic and stratigraphic observations of mounds were primarily made using CaSSIS NPB (Near-Infrared; 'NIR', 850nm, Panchromatic; 'PAN', 650 nm and Blue–Green; 'BLU', 475 nm; Thomas et al., 2017) and HiRISE RED and IRB (infrared-red-blue; McEwen et al., 2007) data. The lower mound boundaries (where the mound-forming material contacts the plains-forming material) were identified in a 6 m/pixel CTX mosaic (Fawdon et al., 2021b) and manually digitized as polygons. Equidistant buffers of 50 m were generated around each mound to represent the surface the mounds are sitting on. This buffer size was selected as it is large enough to capture a representative portion of the mound-adjacent topography from the DTM, and small enough that it reduces the likelihood that other topographically prominent features (e.g. other mounds, craters) could be unintentionally captured in the buffer. Elevation data for all mounds were derived from CTX DTMs (Digital Terrain Models) with a spatial resolution of 20 m/pixel and an expected vertical precision of between 1.34 and 6.16 m (mean 3.19 m; Fawdon et al., 2021b). Using the ArcGIS Pro zonal statistics tool, the maximum elevation of each mound (Z_{apex}) was extracted from the DTM. The median elevation of the topography within the surrounding buffer (Z_{base}) was also extracted to capture the elevation of the surrounding plains. Mound heights were calculated by subtracting Z_{base} from Z_{apex}. These data were encapsulated as a feature class in the GIS, with points generated at the geographic center of each mound that contained the geographic and morphometric information required for further analysis.

To determine whether the Oxia Planum mounds formed part of the larger circum-Chryse mound-forming deposit, we analyzed the volumes and surfaces of this hypothetical layer using the mound morphometric data from this study and from McNeil et al., (2021). From the elevation data, three interpolated surfaces were created using the 3D Analyst tools in ArcGIS Pro (Figure 2). A minimum upper bounding surface (MUBS) was generated from Z_{apex} using the Natural Neighbor tool (which uses the heights and distances between points, weighted by proportional overlaps of constructed Voronoi diagrams, e.g. Sibson, (1981)) to generate a surface. The MUBS is the minimum elevation of the upper surface of the layer from which the mounds originally eroded. The lower bounding surface (LBS) was generated from Z_{base} also using the Natural Neighbor tool, and this represents a generalization of the paleosurface that the mound layer was deposited onto. We used the heights of all mesas and tiered mounds (assumed to be the tallest and most complete sections of the mound-forming deposit) east of Ares Vallis from the database of circum-Chryse mounds in McNeil et al. (2021) to generate a Chryse Planitia upper bounding surface (CPUBS) with the Inverse Distance Weighted surface interpolation tool. The Inverse Distance Weighted tool was required instead of the Natural Neighbor tool to achieve a surface that could be extrapolated to the landing site. The CutFill tool in ArcGIS Pro was used to estimate the volumes bounded by the three interpolated surfaces and the present-day surface described by the CTX DTM (Figure 2b). The volume between the undulating present-day surface and the MUBS is a minimum estimate of the amount of inter-mound material removed from Oxia Planum, and the volume between the present-day surface and the CPUBS is an estimate of the total material that could have been removed assuming the Oxia Planum and Circum-Chryse mounds were originally the same height. The volumes between the LBS and the MUBS, and the LBS and CPUBS, are the minimum amount of removed mound material, and the best estimate of the total removed mound material, respectively. As the present-day surface is below the LBS over significant parts of Oxia Planum, subtracting the present-day surface from the LBS where the mounds are not present yields an estimate of the amount of material eroded from below the base of the mounds. This eroded material may have been mound material and/or clay-bearing unit.

3 Results and Interpretation

3.1 Population Distribution

We have identified 396 mounds within the 8700 km^2 Oxia Planum *Rosalind Franklin* landing site study area. There are 9 mounds (2.3% of the population) within the 2022 1-sigma landing ellipses (Figure 1), and 26 mounds (7.6% of the population) within 3 km of these ellipses. There are 83 individuals (21%) within or partially within the 3-sigma landing ellipse (Figure 1), and a total of 129 (32.6%) examples within 3 km of these ellipses. The mounds cover a total of 0.56% of the study area, 0.16% of the 1-sigma landing ellipse, and 0.88% of the 3-sigma landing ellipse. Assuming that *Rosalind Franklin* lands somewhere in the 1-sigma ellipse, it will be an average of ~2.1 km from a mound, and the furthest it will be from a mound is ~6.0 km. This increases to ~3.7 km (mean) and ~18.6 km (maximum) for the 3-sigma ellipses, but this is highly dependent on exactly where the rover lands in the 3-sigma ellipse; in the northern half of this ellipse the maximum rover-mound distance reduces to 8.1 km. Mounds occur throughout the study area but are more common at lower elevations (Figure S1, S2). As a result, they are also more abundant towards the north and northwest of the landing site (Figure 1, S1), where they appear to become continuous with the mound population seen across the circum-Chryse region. The morphometric and elevation data for the mounds are summarized in Table 1.

3.2 Mound Geology

The mounds are bright-toned and texturally smooth in CTX. In CaSSIS NPB data, they are conspicuous white-yellow features (likely red in true color) that contrast the darker blue and orange tones of the underlying clay-bearing unit (CBU; e.g. Figure 3a). Generally, the tallest parts of mounds appear relatively more white-yellow than the bases, which appear to be more white-blue in HiRISE IRB data. This difference in coloration is consistent in CaSSIS NPB images taken at different times of day, suggesting it is not an effect of illumination. Most mounds are smooth at the meter scale and highly rounded. From orbital data, we have identified three different sub-units (members) associated with mounds in the landing site. The mounds vary considerably in their form, surface texture and color; some mounds exhibit all three members, whereas, in most others, only one or two of the members may be present. As a whole, the mounds are less homogenous than the larger circum-Chryse population, which contain much thicker, stratigraphically continuous deposits of clays (McNeil et al., 2021).

The lower mound member is bright white and blue-toned in CaSSIS NPB and HiRISE IRB data, contains decameter-scale fractures, and sometimes exhibits layering (Figure 3b). This member is exposed in the flanks of mounds where stratigraphically younger material has been eroded away (Figure 3a, b). It is not commonly observed, suggesting that it either does not exist in many mounds, or does exist and is obscured by overlying members. The lower member shares many similarities with the blue member of the CBU including the observation that it is at the same stratigraphic level, contains decameter-scale fractures, has a bluish tone, and does not commonly form prominent topographies (Mandon et al., 2021). Therefore, the lower member may not be true "mound material" but could be prominences of uneroded (or relatively less eroded than the surrounding material) upper sections of the blue CBU (Figure 4). Within the mounds, this member might therefore simply reflect differential erosion of the CBU, where the upper part of the mound has protected the CBU beneath it.

Where it occurs, the middle mound member is always stratigraphically below the upper member (Figure 4). We do not observe the middle member unambiguously in contact with the lower member within any mound, but it always overlies the blue member of the CBU (Figure 3c, d), thus we place it stratigraphically above the lower member. The middle member is not present in all mounds, although we cannot be its true abundance as it is thin (no more than a few meters in thickness), and may be covered by loose material at the bases of mounds in many cases. In CaSSIS NPB, larger exposures are blue in tone, transitioning into yellow tones at the edges and in smaller, more eroded examples (Figure 3d). Where exposed, it is bright and sometimes fractured at the meter-decameter scale in HiRISE (Figures 3, 4), and is similar to the underlying lower member/CBU. The boundary between this member and the blue member of the CBU (and by extension, the lower member) is interpreted to be unconformable, as we observe material interpreted as the middle member in a crater within the blue CBU (Figure 3c); it is, for this reason, we have placed it stratigraphically above the lower member (Figure 4). Some isolated examples of this member appear to have been fractured and completely separated from the main mound (Figure 3d). The middle member also underlies patches of the dark resistant unit (DRU), for example at Germania Lacus (Figure 4f), suggesting the top of the middle member may represent a paleosurface upon which the upper mound unit and DRU were deposited.

The upper mound member is the stratigraphically highest and by implication the youngest mound-forming unit. It has been divided into upper members (part a) and (part b), which share some visual characteristics and occupy approximately the same stratigraphic level in the mound sequence. The upper member is invariably bright yellow-orange in CaSSIS data, and its texture varies between smooth (in the case of upper member (part a); Figures 3c, e, f) and rough (upper member (part b); Figure 5c). There is no clear example of upper member (part a) and upper member (part b) being in direct contact in a single mound, so it is unclear exactly how they are related to each other, and they may be laterally equivalent (Figure 4). Upper member (part b) usually has a much greater thickness than the underlying units and therefore often forms almost the entire topographic extent of the mounds (Figure 3e). Where the lower member and middle member are absent, the upper member is observed to directly contact the CBU (Figure 3, 5). The upper member occurs on the tops, flanks and bases of mounds (e.g. Figure 3b) and also shares a flat boundary with the CBU (e.g. Figure 3e) suggesting that it mantled a paleosurface upon deposition. In HiRISE, the upper member (part b) is layered at the meter- and decameter scale, with all layers being approximately horizontal. Fifteen mounds in this study exhibit clear layering within the upper member at HiRISE scale, with layers often being picked out by boulders (Figure 3e). A mound in the east of the landing site shows rounded, bright-toned, meter-scale boulders defining a basal horizon in otherwise thinner layers which occur in repetitive, ~3 m-thick packages within upper member (part b; Figure 3e). This could be explained by recurring depositional events capable of depositing meter-scale boulders, followed by a drop in energy, and/or a change in the source of the deposit. The bright-toned boulders could be eroded material transported from higher topographies in the Oxia basin, or they could be an erosional feature of the outcrop. The upper member does not have the same polygonal fractures seen in other members, but instead sometimes contains bright, positive-relief linear and curvilinear ridges (Figure 5c, d). These ridges occur primarily on mound surfaces but are also observed to extend into the underlying CBU. One mound (Figure 5c) contains individual upstanding linear features and a triangular section on the northern flank which is bounded by upstanding linear ridges (Figure 5c, d). A set of upstanding linear features intersect the mound at a 60° angle at its apex, resembling conjugate fractures. Another mound in the east of the study area (Figure 5d) exhibits similar curvilinear features. We interpret these features to be surface expressions of erosion-resistant material such as mineralized fractures of sedimentary or igneous origin, that have reinforced the bulk mound structure against erosion (e.g. De Toffoli et al., 2019; Okubo & McEwen, 2007).

3.3 Mound Stratigraphy

3.3.1 Relationship Between Mounds and CBU

The contact between the upper member and CBU is either horizontal or gently dipping throughout the study area, suggesting that the upper member was deposited onto the paleotopography. Given that the upper member also directly overlies both the lower member and the middle member, it is likely that a paleolandscape containing elements of eroded lower member, middle member and CBU was present at the time of the upper member's deposition (Figure 4). Mounds located on the rims of highly eroded, ejecta-free craters that occur within the CBU demonstrate that substantial erosion and time occurred between the impact events (and therefore the CBU formation itself) and the deposition of the mound layer. Malino crater (Figure 1) contains crater-rim mounds and two intra-crater mounds (Figure 5e, f) at similar elevations, suggesting that the mound layer was deposited after both crater infill, and erosion of the crater rim and ejecta. It is unclear how much time elapsed between the CBU formation and emplacement of the mound layer.

Another mound at 18.277°N, 24.523°W shows a horizontal contact ~20 m above the topographic base of the mound (Figure 5b). We interpret this contact as the boundary between the CBU (lower member in this case as it is part of a mound) and the middle member, as it is at a similar elevation relative to the outcrops of the middle member on the west of Germania Lacus (Figure 5g). Below the contact (but still on the topographic mound flank), approximately 20 m of lower member material is exposed. Above the contact, the upper member forms most of the topography of this mound. As such, this is the only landform in the study where all three mound-forming units are unambiguously present.

3.3.2 Relationship Between Mounds and Dark Resistant Unit

The dark resistant unit (DRU) is a dark-toned, rugged unit which occurs throughout the Oxia Planum study area in topographic lows, and as remnant, upstanding mesas. There is no consensus on the origin of the DRU, with both sedimentary and igneous origins proposed (Gary-Bicas & Rogers, 2021; Quantin-Nataf et al., 2021). Its age is also debated; one estimate is early to mid-

Amazonian or older (>2.6 Ga, Quantin-Nataf et al., 2021), and others estimate Early Hesperian (~3.7 Ga; Ivanov et al., 2020; Uthus, 2020).

The DRU onlaps onto a mound in Malino crater, showing that it unconformably overlies the mounds (Figure 5f). Around another intra-crater mound in Malino crater, about 100–200 m of backstepping has occurred (Figure 5e), however, it is not clear whether this is a result of erosion of the DRU, or the mound itself. The erosion in these areas has revealed polygonal fractures in the underlying crater-fill unit, similar to those seen in the CBU.

These relationships show both that the DRU is younger than the mounds, and that the DRU was emplaced after the mounds had been eroded. No evidence has yet been found for hydrous minerals in the DRU (Quantin-Nataf et al., 2021; Carter et al., 2016), whereas several mounds throughout the Chryse region show evidence of hydrous minerals (McNeil et al., 2021), suggesting that a change in environmental conditions occurred between the emplacement of the mound members and DRU. The lack of CRISM data in the area means that the DRU could contain hydrous minerals, but is not detected due to poor coverage.

3.4 Volumetric Calculations of Putative Mound Layer Thickness

To test whether the Oxia Planum mounds could have formed part of the circum-Chryse mound-forming deposit, we calculated the total volume of eroded material which must have been removed to leave the upstanding mounds. In this section, we first assume that the mounds were part of the circum-Chryse layer in order to calculate removed volumes, and then discuss whether this is a realistic hypothesis in section 4. Given that the digitized mound boundaries are the point at which the mound-forming material contacts the material that forms the CBU (lower member in some mounds), the boundaries approximate the stratigraphic position of the middle member (which is extremely thin), and the LBS approximates the paleosurface upon which the middle member rests.

The surface generated by interpolating the mound apexes in the study area (MUBS, Figure 2, S3) reveals a minimum total thickness of eroded mound material in the Oxia Planum study area of 41.4 m, and therefore a minimum volume of 208 km^3 ± 32 km^3 (Table 2) would have had to be removed if the mounds formed from a previously contiguous layer (or layers). This can be subdivided into the minimum eroded depth and volume of the mound-forming layer above the LBS (21.6 m, 124 $km^3 \pm 37\ km^3$), and the eroded depth and volume of the material below the interpolated mound contact or LBS (19.8 m, 84 $km^3 \pm 27\ km^3$). This eroded material is assumed to have been either CBU or lower mound material.

Using the surface generated from the heights of the Chryse Planitia mesas (CPUBS, Figure 2, S2), the estimated total thickness of eroded material in the study area is over three times higher than MUBS at 129 m, with a volume of 680 km^3. This can be subdivided into the eroded thicknesses and volumes of the mound-forming layer (111.6 m, 605 km^3), and the amount of material from below the interpolated lower mound contact or LBS (17.6 m, 75 km^3). The CPUBS intersects the topography in Oxia Planum at an elevation of approximately -2800 m, equivalent to the upper elevation of the Mawrth Plateau deposits to the northeast. Above the CPUBS, which represents the inferred top of the original mound forming layer across both Chryse Planitia and Oxia Planum, there should theoretically be fewer or no mounds found; our observations support this, with only four low-relief mounds having bases above the -2800 m contour. The total volume of mounds in the study area is approximately 1.3 km^3, which is ~1% of the MUBS volume estimate for the study area and 0.21% of the CPUBS volume estimate for the study area.

Based on stratigraphic relationships observed in the wider circum-Chryse mound population, the mounds are likely to have been deposited, indurated, and eroded within approximately 200 Myr, between ~4.0 Ga (the crater retention age of the underlying CBU; Quantin-Nataf et al., 2021, and the time at which the regional Mawrth Vallis plateau was mostly formed; Loizeau et al., 2012) and ~3.8 Ga (the crater retention age of the top of the Mawrth Vallis clay-bearing stratigraphy – and therefore also the circum-Chryse clay-rich deposit – which is correlatable to the youngest parts of mounds in Chryse Planitia). Assuming the Oxia Planum mounds once formed a contiguous part of this circum-Chryse mound-forming deposit and that they are therefore of a similar age, we can estimate the rate of erosion for this deposit in Oxia Planum.

It is unclear what proportion of this time was devoted to deposition versus erosion, or whether the mounds in Oxia Planum were eroded over the same timescales as the larger mounds in Chryse Planitia, so the following calculations of erosion rates are minimum estimates. The minimum thickness of the removed material in Oxia Planum was 41.4 m, and the estimated mean thickness was ~129 m (Table 2). Assuming rapid initial deposition at 4.0 Ga, erosion of these thicknesses at a constant rate for 200 Myr^{-1} equates to a minimum steady-state erosion rate of 0.21–0.65 m Myr^{-1}. Conversely, minimum deposition rates are the same, assuming rapid final erosion.

4 Discussion

4.1 Stratigraphic Implications

The main mound-forming layer (upper member) and the DRU at Germania Lacus both directly overlie the middle member which in turn overlies the lower member/CBU. We interpret the boundary between the middle member and upper member to represent a paleosurface which existed at the time of deposition of both the upper member and the DRU. The middle member is extremely thin, and its presence underneath highly eroded remnants of both the upper member and DRU (Figure 5g) could suggest that it remained relatively unchanged in the time between the deposition of the upper member and DRU. By extension, this could imply that DRU is more ancient than previously thought and could be closer in age to the early Hesperian estimated by Ivanov et al. (2020) and Uthus (2020) than the early Amazonian lower limit in Quantin-Nataf et al. (2021). Therefore, it is possible that the DRU is genetically related to the extensive dark plains material which occurs throughout Chryse Planitia (~3.6 Ga, Loizeau et al., 2012, Tanaka et al., 2005) and embays mounds (McNeil et al., 2021), as postulated in Quantin-Nataf et al, (2021).

4.2 Constructional Isolated Features, or Erosional Layer-Derived Landforms?

This section discusses whether the mounds are constructional (their morphologies formed in isolation from each other through the progressive build-up of material) or if they are erosional (their morphologies formed through erosion of a previously more extensive layer or layers).

The strongest evidence that supports mound formation through erosional processes, and that the mounds were once more extensive than they are today, comes from the structure and stratigraphy of the mounds:

(1) Mounds in the Oxia Planum population are all composed of the same internal stratigraphy; the upper, middle, and lower members occur in the same succession and are of similar relative thicknesses where they are present (Figure 3).

(2) The lower member and the middle member are composed of similar material (in both color and texture) to the clay-bearing unit (Figure 3c, d) that surrounds the mound landforms. Because the only difference between 'plains' and 'mounds' is the slope of the rock exposure, this strongly suggests that the lower sections of mounds are less eroded parts of the clay-bearing unit (Figure 5b, h), which have been eroded relative to the mounds.

(3) The upper member of the mound stratigraphy that forms steeply dipping and rounded flanks are consistently covered in material that mostly obscures other elements of the internal mound structure (Figure 3b) on the flanks. This is most consistent with scree slopes suggesting ongoing erosion. Whilst this overall form is not inconsistent with constructional landforms, if the origin was constructional then the covering material would need to be actively replaced by that constructional process, to maintain their shape over geological time.

These observations show that the mounds comprise multiple distinct layered members, some of which appear to be separated by unconformities and thus record substantial amounts of geologic time. This stratigraphic consistency and erosional environment support the interpretation that the layers were previously continuous between the mounds. Furthermore, this evidence reduces the likelihood that they are constructional in nature, as any constructional process would have had to independently reproduce the same members at consistent thicknesses at different points in space.

Outside the study area (geographically focused by our science questions) the population of mounds is continuous with those in Chryse Planitia. The origin of mounds in Oxia Planum must be consistent with the rest of this population because:

(1) There is no sudden change in the tone, brightness, size or shape characteristics between mounds in Oxia and those nearby in the circum-Chryse region; there is an overall gradual increase in size to the north, consistent with a layer of increasing thickness and/or increased erosion to the north.

(2) The top of the extrapolated circum-Chryse upper bounding surface forms a slope of low gradient which overlays the entire Oxia Planum population. This is what we would expect if the Oxia Planum mounds represented smaller examples of the circum-Chryse mound deposit described in McNeil et al. (2021).

(3) Clusters of partially dissected mounds (Figure 3a) illustrate an evolutionary sequence from larger plateaus through clusters of mounds to increasingly isolated features (e.g.; Figure 5h).

Additional contextual evidence precludes the survival of small constructional landforms over geological time: the mounds are in a region with multitudes of other erosional landforms such as inverted channels (Fawdon et al., 2021a, b; Davis et al., 2022), inverted craters (Quantin-Nataf et al., 2021; Roberts et al., 2021), Periodic Bedrock Ridges (Favaro et al., 2021; Silvestro et al., 2021), and the DRU (Fawdon et al., 2021b; Quantin-Nataf et al., 2021). These, along with the low surface dust index (Ruff & Christensen, 2002) and population of aeolian bedforms indicative of transport over a long period of time (Favaro et al., 2021), are indicative of an erosive environment in Oxia Planum. This is consistent with an erosional origin, and inconsistent with the survival of isolated constructional landforms, which, given their relationship to the DRU, must have predated the substantial amount of erosion that has affected that unit (Figure 5b); consequently it is not plausible that they would have simultaneously predated this erosive environment and have been substantially unaffected by it.

In addition to the evidence consistent with an erosional origin, there is a lack of evidence to support common processes that construct isolated, mound-like landforms. There is no geomorphologic evidence to indicate that these mounds are volcanic in origin; they do not look like other small-scale volcanic features from Mars, either igneous (Brož & Hauber, 2012, 2013; Brož et al., 2014) or sedimentary (Brož et al., 2019, 2022; Oehler & Allen, 2010) in origin, and we see no evidence for features typical of these processes such as summit craters, conical morphologies, or igneous mineralogy. There are no instances associated with flow-like landforms on their flanks and we do not observe any regionally-contextual volcanic architecture of comparable age or apparent preservation.

The mounds could also be hydrothermal in origin. However, we do not observe any evidence of vents or bright outcrops (Skok et al., 2010) or the context of a long-lived volcanic system (e.g. Fawdon et al., 2015), nor do we see mineral assemblages associated with hydrothermalism (e.g. serpentine, chlorite) in hyperspectral CRISM data in the Oxia Planum region (Mandon et al., 2021; Skok et al., 2010). Some mounds contain what appear to be linear resistant ridges (Figure 5c, d) which could be interpreted as dykes of intrusive material, but given the lack of contextual volcanic architecture, these are more simply interpreted as mineralised fractures – commonly seen in martian terrains (Caswell & Milliken, 2017; Okubo & McEwen, 2007) – which are exposed in more eroded parts of the mounds. Although this doesn't support a constructional origin, it does mean that hydrothermal mineralisation could have been a significant factor in preserving the mounds. Furthermore, the lack of supporting mineralogy may be attributed to a combination of dust coverage, the small area of bedrock exposed on mound surfaces, and a lack of quality data coverage.

Either a hydrothermal and a volcanic/sedimentary volcanic origin for the mounds would require a prolonged and regionally extensive thermal source, which could be provided from a mantle plume or the residual energy from a prior large impact. The former is unlikely, given the lack of obvious large-scale volcanic landforms in the region, however the latter is superficially more plausible. Chryse Planitia is comparable in size (diameter: ~1500 km) to other large impact basins on Mars, such as Hellas (diameter: ~2000 km), which are likely to have produced hydrothermal systems at the rims and central peak that may have been sustained for ~10 Myr after the impact events (Abramov & Kring, 2005). Oxia Planum is located at the edge of the Chryse basin near its proposed rim (e.g. Pan et al., 2019), so there is circumstantial evidence the region may have been subjected to hydrothermal activity in the tens of millions of years after the impact. However, it is unclear if this is stratigraphically consistent with the timing of deposition and/or alteration of the CBU in Oxia Planum and the wider circum-Chryse clays (Brossier et al., 2022; Carter et al., 2015; Mandon et al., 2021).

On balance, we suggest there is substantially more evidence, requiring fewer special circumstances, that the mounds formed from erosional processes eroding one or more layers of pre-existing material. We find little to no direct or contextual evidence to support constructional processes, and whilst there is no irrefutable evidence to rule out a constructional hypothesis the observations are commensurate with the current mound morphology being primarily erosional in nature.

4.3 Wider Implications

Mounds in the Oxia Planum region are smaller (in height and diameter) than most of the mounds in the wider circum-Chryse region. It is unclear whether this is primarily because the mound-forming layer was thinner in Oxia Planum, or if more erosion occurred here, or a combination of the two. Given that CPUBS predicts a thinner layer in Oxia Planum, and that this surface was constructed using mesas (thought to be the most complete sections of the mound-forming stratigraphy; McNeil et al. 2021), we favor the hypothesis that the mound-forming layer was thinner in Oxia Planum, or that the mounds represent three-dimensional exposures of the top of the clay-bearing succession in this region of Chryse Planitia. If the former is true, the thinning of the mound-forming layer towards the basin margin implies constraints on its formation mechanism. Thinner deposits at basin margins are a common feature of sedimentary basins on Earth, where the accumulated sediment thickness decreases towards the basin margin as accommodation space decreases. Furthermore, meter-scale layering in the Oxia Planum mounds could be consistent with deposition through sedimentary or ashfall processes whose thickness across a basin is usually influenced by accommodation space.

4.4 Deposition and Overburden Removal in Oxia Planum: Rates and Timing

Our calculated minimum deposition/erosion rates are similar to previous estimates of middle-late Noachian global erosion rates (0.8 – 1 m My^{-1}, see summary in Golombek et al., 2006), and are considerably lower than previous crater obliteration estimates for Oxia Planum itself (8 m My^{-1}, Quantin-Nataf et al., 2021). Our estimates differ from those in Quantin-Nataf et al., (2021) primarily because our estimates are for the minimum mean erosion rates, whereas theirs are mean crater obliteration rates (which is the rate at which craters are removed through both deposition and erosion). Our calculated erosion rates are a similar order of magnitude but lower than the median erosion rate of outcrops in arid to polar environments on Earth (~6 m My^{-1}; Portenga & Bierman, 2011), which is perhaps not surprising given the different atmospheric conditions. However, Amazonian estimates for erosion rates in Oxia Planum are much lower: 0.01 – 0.03 m My^{-1} (Kite & Mayer, 2017) and 0.08 m My^{-1} (Quantin-Nataf et al., 2021). The difference between these Amazonian rates and our minimum rates supports our interpretation that most of the mound material erosion took place in the Noachian/Hesperian rather than during the Amazonian.

Assuming an average Noachian erosion rate of approximately 0.9 m My^{-1} (Golombek et al. 2006), this would mean that the estimated ~130 m of mound material would have been removed in ~150 Myr before embayment by the dark plains material. Deposition would have had to occur over the prior ~50 Myr, with an average rate of approximately 2.6 m My^{-1}, similar to Holocene sedimentation rates in some of the deepest parts of Earth's oceans (Piñero et al., 2013). The true erosion and deposition rates are likely to be more complex, with alternating periods of deposition, erosion and inactivity, as indicated by the layering in some mounds (Figure 3e). Factors that could affect the depositional and erosion regime include sediment availability and source, environmental conditions that would influence the amount highland runoff, and impact gardening, amongst others. Furthermore, we do not know how early Martian environmental conditions including putative ocean chemistry might have affected these deposition rates. Mound-derived TARs (Transverse Aeolian Ridges; Balme et al., 2008) around the bases of mounds and across the study area (Favaro et al., 2021) demonstrate that sediment transport, and thus probably also wind erosion, is occurring here at the present time.

4.5 Implications for the Landing Site and *Rosalind Franklin*

Our calculations show that the clay-bearing plains unit in the landing site of the *Rosalind Franklin* rover was buried by ~130 m of overburden during the Noachian – an order of magnitude shallower burial than calculated by Quantin-Nataf et al., (2021). Hydraulic fracturing of rocks on Mars has been calculated to occur at depths of one kilometer or greater (Caswell & Milliken, 2017), so the vertical stress imparted to the CBU from ~130 m of overlying material alone is unlikely to have been great enough to produce the fractures seen in the CBU. The maximum thickness of the mound-forming layer in Chryse Planitia was around 550 m (McNeil et al., 2021), or around half of what would be needed to fracture the underlying bedrock. It seems unlikely therefore from our reconstruction that Oxia Planum, which is closer to the edge of the Chryse basin, would be able to accommodate twice the thickness of material than deeper areas of the basin – especially when the evidence presented here suggests that the layer was considerably thinner in Oxia Planum. There are two possibilities: 1) hydraulic fracturing of the CBU was the result of deformation of an underlying ductile layer (Quantin-Nataf et al., 2021); or 2) fractures in the CBU are not hydraulic but are the result of horizontal tensile stresses generated by contractional processes such as desiccation, syneresis, or thermal contraction (Parkes Bowen et al., 2022). Identification and analysis of sub-HiRISE-scale mound-proximal fractures in the CBU using the PanCam instrument aboard the *Rosalind Franklin* rover (Coates et al., 2017) could allow for a better understanding of their origins.

The similarities in height difference between the top of the present-day mounds and the paleosurface defined by the contact between the mounds and CBU suggest that when the mound layer was emplaced in the Noachian, the geography of Oxia Planum was broadly comparable with its modern low-relief topography. Despite this, there are small differences, as the geological boundary often occurs near the base of the topographic mound slope (e.g. Figure 5b) suggesting that these mounds have protected a more complete section of the CBU.

The mounds appear to be the second-oldest unit in the landing site after the CBU. Therefore, the regions of CBU that occur directly below still-intact mounds have remained buried and unexposed since burial in the early-middle Noachian and have had greater protection from solar radiation, impact events, and atmospheric alteration than exposed CBU. Any potential biosignatures would also have been afforded this protection. The mounds also could record water-rock interaction as their upstanding lineations are interpreted as indurated fractures, suggesting interaction with fluids (McNeil et al., 2021). We propose that the base of mounds – particularly tall, layered mounds with indurated fractures that show evidence of active erosion – and subordinately, areas around DRU mesas, may be among the best places in the landing ellipses to detect biosignatures in the CBU.

It is feasible that the *Rosalind Franklin* rover will land close enough to a mound to be able to image it in situ with the PanCam instrument, including the HRC (High Resolution Camera) and WAC (Wide Angle Cameras; Coates et al., 2017). Ground-based imaging of strata exposed on individual mound edifices could allow us to determine the depositional environments in which the mound-forming unit was formed, for example by identifying sedimentological features such as clast size, geometry and orientation, horizontal- and cross-stratification, scours, channels or grading. Whilst the sedimentology and stratigraphy of individual mounds will be able to inform us about the origin of the deposits, images of multiple mounds will allow for a better understanding of the wider mound-forming deposit and could elucidate whether it was deposited through primary deposition, ashfall processes, the reworking of pre-existing material, or any combination of these. If the mounds were part of a regional layer, we would expect to be able to see consistent sedimentological features across different examples, and we would also expect a compositional difference between the upper member and the lower member/middle member. If the mounds are distal outliers of Oxia Planum (Coogoon Valles) sediment fan material (e.g. Quantin-Nataf et al., 2021) or progradation of any highland detrital sediments, we might expect to see large-scale sedimentary features exposed in mound flanks. The *Perseverance* and *Curiosity* rovers both imaged the flanks of Kodiak Butte and the Murray Buttes in their respective landing sites, revealing large-scale sedimentary features which have contributed to our understanding of past depositional environments in these locations (e.g. Banham et al., 2021; Mangold et al., 2021). Similar analyses using PanCam data from the *Rosalind Franklin* rover may allow for an improved understanding of the Noachian environments of Oxia Planum.

5 Conclusions

- The morphology of mounds in Oxia Planum is more likely to be the result of erosional processes than constructional processes. The Oxia mounds are morphologically and morphometrically continuous with the population of larger mounds further out in the Chryse basin, and comprised part of a Noachian-aged, layered deposit that extended around the circum-Chryse region.
- The mounds contain as many as three distinct members, possibly separated by unconformities: the lower mound member, a bright, layered, blue-toned material, which could be uneroded sections of the uppermost clay-bearing plains; the middle mound member, a thin, low-relief blue-toned material; and the upper mound member, a yellow-toned material of variable roughness which forms most of the mound topography.
- In Oxia Planum, the mound-forming layer had a minimum mean thickness of ~40 m but is likely to have had a mean thickness of ~130 m. This is considerably thinner than elsewhere in Chryse Planitia, suggesting that the mound-forming layer thinned towards Arabia Terra to the south, following the elevation of both the paleosurface and the present-day elevation. Alternatively, the Oxia Planum mounds may represent the uppermost part of the circum-Chryse mound-forming deposit.
- Our minimum erosion rate estimates are an order of magnitude higher than Amazonian estimates, a similar order of magnitude but slightly lower than present-day erosion rates in arid and polar deserts on Earth, and comparable to previous estimates of erosion rates on Noachian Mars.
- Mounds in Oxia Planum show positive-relief linear to curvilinear features that are similar to examples in the circum-Chryse region. These are interpreted to be indurated fractures, suggesting interaction with fluids and precipitation of resistant minerals.

- It is highly unlikely that the mound-forming layer alone provided enough vertical stress to hydraulically fracture the clay-bearing unit, suggesting either that the overburden in the region was considerably thicker than our calculations suggest, or that hydraulic fracturing was achieved through non-overburden-induced stress, or that the fractures were formed 'near-surface' through horizontal tensile stresses.
- Those areas of the clay-bearing plains which are directly covered by mounds have been continually protected from the martian environment since the Noachian, and are likely to be the most pristine clay-rich materials in the landing site. The areas directly adjacent to the mounds (and mesas of dark resistant material), are likely to have been more recently exposed than other areas away from the mounds through the erosion and backstepping of these younger units. These are therefore the most promising locations for *Rosalind Franklin* to search for subsurface biosignatures.
- In situ imaging of the flanks of mounds by Rosalind Franklin's PanCam instrument is likely to help reveal the origin of the mound material, and aid in our understanding of the early martian depositional environments present in Oxia Planum.

Acknowledgements

JDM acknowledges STFC for support under Doctoral Training Grant SA215664, and the Open University SRA. MRB and PF acknowledge UK Space Agency Funding: ST/V001965/1, ST/R001413/1 and ST/W002736/1. An anonymous reviewer, Solmaz Adeli, Daniela Tirsch, Thomas Früh, Kristen Bennett, and the editors Andrew Dombard and Bradley Thomson, are thanked for their insightful comments which greatly helped to improve this manuscript. The authors wish to thank the CaSSIS spacecraft and instrument engineering teams. CaSSIS is a project of the University of Bern and funded through the Swiss Space Office via ESA's PRODEX programme. The instrument hardware development was also supported by the Italian Space Agency (ASI) (ASI-INAF agreement no. I/2020-17-HH.0), INAF/Astronomical Observatory of Padova, and the Space Research Center (CBK) in Warsaw. Support from SGF (Budapest), the University of Arizona (Lunar and Planetary Lab.) and NASA are also gratefully acknowledged. Operations support from the UK Space Agency under grant ST/R003025/1 is also acknowledged.

Open Research

Supplementary information including tabulated mound morphometric and location data as well as geospatial data vectors (shapefiles, .shp) for mounds are available in McNeil et al. (2021). See supplementary materials for supporting figures and tables. CTX and HiRISE image data are publicly available at the NASA Planetary Data System repository in the Mars Reconnaissance Orbiter section (https://pds-imaging.jpl.nasa.gov/volumes/mro.html). CaSSIS data are publicly available at the ESA Planetary Science Archive (European Space Agency, 2021a) and (European Space Agency, 2021b), with relevant Oxia Planum-specific CaSSIS data available at Fawdon et al., (2021c). CaSSIS observations are also available at https://cassis.halimede.unibe.ch/observations. A guide to downloading and viewing CaSSIS data is available at https://issues.cosmos.esa.int/socciwiki/display/PSAPUB1/CaSSIS+Quick+Start+Guide.

References

Abramov, O., & Kring, D. A. (2005). Impact-induced hydrothermal activity on early Mars. *Journal of Geophysical Research E: Planets*, *110*(12), 1–19. https://doi.org/10.1029/2005JE002453

Balme, M., Berman, D. C., Bourke, M. C., & Zimbelman, J. R. (2008). Transverse Aeolian Ridges (TARs) on Mars. *Geomorphology*, *101*(4), 703–720. https://doi.org/10.1016/j.geomorph.2008.03.011

Banham, S. G., Gupta, S., Rubin, D. M., Edgett, K. S., Barnes, R., Van Beek, J., et al. (2021). A Rock Record of Complex Aeolian Bedforms in a Hesperian Desert Landscape: The Stimson Formation as Exposed in the Murray Buttes, Gale Crater, Mars. *Journal of Geophysical Research: Planets*, *126*(4). https://doi.org/10.1029/2020JE006554

Bibring, J.-P., Soufflot, A., Berthé, M., Langevin, Y., Gondet, B., Drossart, P., et al. (2004). OMEGA: Observatoire pour la Minéralogie, l'Eau, les Glaces et l'Activité (Vol. 1240, pp. 37–49). Presented at the Mars Express: the scientific payload.

Brossier, J., Altieri, F., De Sanctis, M. C., Frigeri, A., Ferrari, M., De Angelis, S., et al. (2022). Constraining the spectral behavior of the clay-bearing outcrops in Oxia Planum, the landing site for ExoMars "Rosalind Franklin" rover. *Icarus*, *386*, 115114. https://doi.org/10.1016/j.icarus.2022.115114

Brož, P., & Hauber, E. (2012). A unique volcanic field in Tharsis, Mars: Pyroclastic cones as evidence for explosive eruptions. *Icarus*, *218*(1), 88–99. https://doi.org/10.1016/j.icarus.2011.11.030

Brož, P., & Hauber, E. (2013). Hydrovolcanic tuff rings and cones as indicators for phreatomagmatic explosive eruptions on Mars: PHREATOMAGMATIC ERUPTIONS ON MARS. *Journal of Geophysical Research: Planets*, *118*(8), 1656–1675. https://doi.org/10.1002/jgre.20120

Brož, P., Hauber, E., van de Burgt, I., Špillar, V., & Michael, G. (2019). Subsurface Sediment Mobilization in the Southern Chryse Planitia on Mars. *Journal of Geophysical Research: Planets*, *124*(3), 703–720. https://doi.org/10.1029/2018JE005868

Brož, P., Hauber, E., Conway, S. J., Luzzi, E., Mazzini, A., Noblet, A., et al. (2022). New evidence for sedimentary volcanism on Chryse Planitia, Mars. *Icarus*, *382*, 115038. https://doi.org/10.1016/j.icarus.2022.115038

Brož, Petr, Čadek, O., Hauber, E., & Rossi, A. P. (2014). Shape of scoria cones on Mars: Insights from numerical modeling of ballistic pathways. *Earth and Planetary Science Letters*, *406*, 14–23. https://doi.org/10.1016/j.epsl.2014.09.002

Carter, J., Loizeau, D., Quantin, C., Balme, M., Poulet, F., Gupta, S., et al. (2015). Mineralogic context of the circum-Chryse Planitia candidate landing sites for the ExoMars Rover mission (Vol. 1988). Presented at the 46th Lunar and Planetary Science Conference.

Carter, J., Quantin, C., Thollot, P., Loizeau, D., Ody, A., Lozach, L., et al. (2016). Oxia Planum, A Clay-laden Landing Site Proposed For The Exomars Rover Mission: Aqueous Mineralogy And Alteration Scenarios. (Vol. The Woodlands, Texas, p. 2). Presented at the 47th Lunar and Planetary Science Conference, The Woodlands, Texas.

Caswell, T. E., & Milliken, R. E. (2017). Evidence for hydraulic fracturing at Gale crater, Mars: Implications for burial depth of the Yellowknife Bay formation. *Earth and Planetary Science Letters*, *468*, 72–84. https://doi.org/10.1016/j.epsl.2017.03.033

Coates, A. J., Jaumann, R., Griffiths, A. D., Leff, C. E., Schmitz, N., Josset, J.-L., et al. (2017). The PanCam Instrument for the ExoMars Rover. *Astrobiology*, *17*(6–7), 511–541. https://doi.org/10.1089/ast.2016.1548

Davis, J. M., Balme, M. R., Fawdon, P., Grindrod, P. M., Favaro, E. A., Banham, S. G., & Thomas, N. (2022). *Ancient Alluvial Plains at Oxia Planum, Mars* (preprint). Planetology. https://doi.org/10.1002/essoar.10511552.1

De Toffoli, B., Mangold, N., Massironi, M., Pozzobon, R., Mouélic, S. L., L'Haridon, J., & Cremonese, G. (2019). Fluid migration through fracture networks, Gale crater (Mars). In *Geophysical Research Abstracts* (Vol. 21., pp. 1-1.1).

European Space Agency (2021a). ExoMars 2016 CaSSIS Raw-level Data Product Collection, 2.2 [Dataset]. https://doi.org/10.5270/esa-lsglomt

European Space Agency (2021b). ExoMars 2016 CaSSIS calibrated Data Product Collection, 2.2 [Dataset]. https://doi.org/10.5270/esa-da0ic0t

Favaro, E. A., Balme, M. R., Davis, J. M., Grindrod, P. M., Fawdon, P., Barrett, A. M., & Lewis, S. R. (2021). The Aeolian Environment of the Landing Site for the ExoMars Rosalind

Franklin Rover in Oxia Planum, Mars. *Journal of Geophysical Research: Planets*, *126*(4). https://doi.org/10.1029/2020JE006723

Fawdon, P., Skok, J. R., Balme, M. R., Vye- Brown, C. L., Rothery, D. A., & Jordan, C. J. (2015). The geological history of Nili Patera, Mars. *Journal of Geophysical Research: Planets*, *120*(5), 951–977. https://doi.org/10.1002/2015JE004795

Fawdon, Peter, Balme, M. R., Davis, J. M., Bridges, J. C., Gupta, S., & Quantin-Nataf, C. (2021a). Rivers and Lakes in Western Arabia Terra: The Fluvial Catchment of the ExoMars 2022 rover landing site. *Earth and Space Science Open Archive*, 47. https://doi.org/10.1002/essoar.10507896.1

Fawdon, Peter, Grindrod, P., Orgel, C., Sefton-Nash, E., Adeli, S., Balme, M., et al. (2021b). The geography of Oxia Planum. *Journal of Maps*, *17*(2), 621–637. https://doi.org/10.1080/17445647.2021.1982035

Fawdon, P., Grindrod, P., Orgel, C., Sefton-Nash, E., Adeli, S., Balme, M., et al. (2021c). The Geography of Oxia Planum 02 CASSIS Data [Dataset]. The Open University. https://doi.org/10.21954/OU.RD.16451217.V1

Gary-Bicas, C. E., & Rogers, A. D. (2021). Geologic and Thermal Characterization of Oxia Planum Using Mars Odyssey THEMIS Data. *Journal of Geophysical Research*, 27.

Golombek, M. P., Grant, J. A., Crumpler, L. S., Greeley, R., Arvidson, R. E., Bell, J. F., et al. (2006). Erosion rates at the Mars Exploration Rover landing sites and long-term climate change on Mars: CLIMATE CHANGE FROM THE MARS ROVERS. *Journal of Geophysical Research: Planets*, *111*(E12), n/a-n/a. https://doi.org/10.1029/2006JE002754

Ivanov, M. A., Slyuta, E. N., Grishakina, E. A., & Dmitrovskii, A. A. (2020). Geomorphological Analysis of ExoMars Candidate Landing Site Oxia Planum. *Solar System Research*, *54*(1), 1–14. https://doi.org/10.1134/S0038094620010050

Jaumann, R., Neukum, G., Behnke, T., Duxbury, T. C., Eichentopf, K., Flohrer, J., et al. (2007). The high-resolution stereo camera (HRSC) experiment on Mars Express: Instrument aspects and experiment conduct from interplanetary cruise through the nominal mission. *Planetary and Space Science*, *55*(7–8), 928–952. https://doi.org/10.1016/j.pss.2006.12.003

Kite, E. S., & Mayer, D. P. (2017). Mars sedimentary rock erosion rates constrained using crater counts, with applications to organic-matter preservation and to the global dust cycle. *Icarus*, *286*, 212–222. https://doi.org/10.1016/j.icarus.2016.10.010

Loizeau, D., Werner, S. C., Mangold, N., Bibring, J. P., & Vago, J. L. (2012). Chronology of deposition and alteration in the Mawrth Vallis region, Mars. *Planetary and Space Science*, *72*(1), 31–43. https://doi.org/10.1016/j.pss.2012.06.023

Malin, M. C., Bell, J. F., Cantor, B. A., Caplinger, M. A., Calvin, W. M., Clancy, R. T., et al. (2007). Context Camera Investigation on board the Mars Reconnaissance Orbiter. *Journal of Geophysical Research E: Planets*, *112*(5), 1–25. https://doi.org/10.1029/2006JE002808

Mandon, L., Parkes Bowen, A., Quantin-Nataf, C., Bridges, J. C., Carter, J., Pan, L., et al. (2021). Morphological and Spectral Diversity of the Clay-Bearing Unit at the ExoMars Landing Site Oxia Planum. *Astrobiology*, *21*(4), 464–480. https://doi.org/10.1089/ast.2020.2292

Mangold, N., Gupta, S., Gasnault, O., Dromart, G., Tarnas, J. D., Sholes, S. F., et al. (2021). Perseverance rover reveals an ancient delta-lake system and flood deposits at Jezero crater, Mars. *Science*, *374*(6568), 711–717. https://doi.org/10.1126/science.abl4051

McEwen, A. S., Eliason, E. M., Bergstrom, J. W., Bridges, N. T., Hansen, C. J., Delamere, W. A., et al. (2007). Mars reconnaissance orbiter's high resolution imaging science experiment (HiRISE). *Journal of Geophysical Research E: Planets*, *112*(5), 1–40. https://doi.org/10.1029/2005JE002605

McNeil, J. D., Fawdon, P., & Balme, M. R. (2021). Morphology, Morphometry and Distribution of Isolated Landforms in Southern Chryse Planitia, Mars. *Journal of Geophysical Research*, 23.

McNeil, J. D; Fawdon, P.; Balme, M.; Coe, A.L. (2021). Oxia Planum ExoMars 2022 Rover Landing Site Mounds: Morphometric Data. The Open University. Dataset. https://doi.org/10.21954/ou.rd.16832266.v2

Molina, A., López, I., Prieto-Ballesteros, O., Fernández-Remolar, D., de Pablo, M. Á., & Gómez, F. (2017). Coogoon Valles, western Arabia Terra: Hydrological evolution of a complex Martian channel system. *Icarus*, *293*, 27–44. https://doi.org/10.1016/j.icarus.2017.04.002

Murchie, S., Arvidson, R., Bedini, P., Beisser, K., Bibring, J. P., Bishop, J., et al. (2007). Compact Connaissance Imaging Spectrometer for Mars (CRISM) on Mars Reconnaissance Orbiter (MRO). *Journal of Geophysical Research E: Planets*, *112*(5), 1–57. https://doi.org/10.1029/2006JE002682

Oehler, D. Z., & Allen, C. C. (2010). Evidence for pervasive mud volcanism in Acidalia Planitia, Mars. *Icarus*, *208*(2), 636–657. https://doi.org/10.1016/j.icarus.2010.03.031

Okubo, C. H., & McEwen, A. S. (2007). Fracture-Controlled Paleo-Fluid Flow in Candor Chasma, Mars. *Science*, *315*(5814), 983–985. https://doi.org/10.1126/science.1136855

Pan, L., Quantin-Nataf, C., Breton, S., & Michaut, C. (2019). The impact origin and evolution of Chryse Planitia on Mars revealed by buried craters. *Nature Communications*, *10*(1), 1–8. https://doi.org/10.1038/s41467-019-12162-0

Parkes Bowen, A. P., Bridges, J., Tornabene, L., Mandon, L., Quantin-Nataf, C., Patel, M. R., et al. (2022). A CaSSIS and HiRISE map of the Clay-bearing Unit at the ExoMars 2022 landing site in Oxia Planum. *Planetary and Space Science*, *214*, 105429. https://doi.org/10.1016/j.pss.2022.105429

Piñero, E., Marquardt, M., Hensen, C., Haeckel, M., & Wallmann, K. (2013). Estimation of the global inventory of methane hydrates in marine sediments using transfer functions. *Biogeosciences*, *10*(2), 959–975. https://doi.org/10.5194/bg-10-959-2013

Portenga, E. W., & Bierman, P. R. (2011). Understanding Earth's eroding surface with 10Be. *GSA Today*, *21*(8), 4–10. https://doi.org/10.1130/G111A.1

Quantin-Nataf, C., Carter, J., Mandon, L., Thollot, P., Balme, M., Volat, M., et al. (2021). Oxia Planum: The Landing Site for the ExoMars "Rosalind Franklin" Rover Mission: Geological Context and Prelanding Interpretation. *Astrobiology*, *21*(3), 345–366. https://doi.org/10.1089/ast.2019.2191

Roberts, A. L., Fawdon, P., & Mirino, M. (2021). Impact crater degradation, Oxia Planum, Mars. *Journal of Maps*, *17*(2), 569–578.

Ruff, S. W., & Christensen, P. R. (2002). Bright and dark regions on Mars: Particle size and mineralogical characteristics based on Thermal Emission Spectrometer data. *Journal of Geophysical Research: Planets*, *107*(E12), 2-1-2–22. https://doi.org/10.1029/2001JE001580

Sibson, R. (1981). A brief description of natural neighbour interpolation. *Interpreting Multivariate Data*.

Silvestro, S., Pacifici, A., Salese, F., Vaz, D. A., Neesemann, A., Tirsch, D., et al. (2021). Periodic Bedrock Ridges at the ExoMars 2022 Landing Site: Evidence for a Changing Wind Regime. *Geophysical Research Letters*, *48*(4). https://doi.org/10.1029/2020GL091651

Skok, J. R., Mustard, J. F., Ehlmann, B. L., Milliken, R. E., & Murchie, S. L. (2010). Silica deposits in the Nili Patera caldera on the Syrtis Major volcanic complex on Mars. *Nature Geoscience*, *3*(12), 838–841. https://doi.org/10.1038/ngeo990

Smith, D. E., Zuber, M. T., Frey, H. V., Garvin, J. B., Head, J. W., Muhleman, D. O., et al. (2001). Mars Orbiter Laser Altimeter: Experiment summary after the first year of global mapping of Mars. *Journal of Geophysical Research: Planets*, *106*(E10), 23689–23722. https://doi.org/10.1029/2000JE001364

Tanaka, K. L., Skinner, J. A., & Hare, T. M. (2005). Geologic Map of the Northern Plains of Mars. *U.S. Geological Survey Geologic Investigations*, *SIM 2888*, 80225–80225.

Thomas, N., Cremonese, G., Ziethe, R., Gerber, M., Brändli, M., Bruno, G., et al. (2017). The Colour and Stereo Surface Imaging System (CaSSIS) for the ExoMars Trace Gas Orbiter. *Space Science Reviews*, *212*(3–4), 1897–1944. https://doi.org/10.1007/s11214-017-0421-1

Uthus, T. N. (2020). *Crater statistics and Geological history of Oxia Planum, landing site for ExoMars2022*. University of Oslo.

Vago, J. L., Westall, F., Coates, A. J., Jaumann, R., Korablev, O., Ciarletti, V., et al. (2017). Habitability on Early Mars and the Search for Biosignatures with the ExoMars Rover. *Astrobiology*, *17*(6–7), 471–510. https://doi.org/10.1089/ast.2016.1533

Figure 1: Mounds in the Oxia Planum region, showing: a) the location of mounds in the study area relative to ~14,000 mounds (white) in the circum-Chryse region; background of MOLA (Mars Orbiter Laser Altimeter; Smith et al., 2001) and HRSC (High Resolution Stereo Camera; Jaumann et al., 2007) hillshade, TV: Tiu Valles, AV: Ares Valles, MV: Mawrth Vallis, b) 2x exaggerated 3D HiRISE image of a typical mound (ESP_039299_1985), showing its prominence over the surrounding clay-bearing unit (CBU) and dark resistant unit (DRU), and c) CTX DTM (digital terrain model) of 396 mounds (white) and the 1-sigma (green) and 3-sigma (yellow) landing ellipses, GL: Germania Lacus, KC: Kilkhampton Crater. The panels in Figures 3 and 4 are labelled in cyan.

Figure 2: Schematic transects across Chryse Planitia and Oxia Planum, showing a) surfaces generated from mound elevation data (CPUBS; Chryse Planitia Upper Bounding Surface, MUBS; Minimum Upper Bounding Surface, and LBS; Lower Bounding Surface), the relationships between the mounds, clay-bearing unit (CBU) and dark resistant unit (DRU), and b) close-up of a mound in Oxia Planum showing the interplay between surfaces and resultant calculated volumes. Dashed lines indicate interpolated surfaces; circles indicate known elevation points used in surface construction. Most Oxia Planum mounds are classified as hills in McNeil et al., (2021) owing to their rounded tops.

Figure 3: Observations of different component mound members throughout the landing site and wider Oxia Planum area; a) HiRISE IRB [ESP_057747_1985] showing a cluster of mounds around a larger, dissected mound (gullies shown by dotted lines) north of Germania Lacus, where the rough, yellow upper member (UM) covers a blue-white toned lower member (LM), which we suggest is uneroded sections of blue member of the CBU; b) exposed layering (red dotted lines) within the lower member; c) CaSSIS [MY36_016481_161_0] showing a cluster of mounds southwest of the study area showing two mounds with the upper member overlying middle member (MM) on the blue member of the CBU, isolated patches of middle member (white arrows), and a potential unconformity shown by possible middle member (due to similar color and texture) infilling craters within the blue member of the CBU; d) CaSSIS [MY36_018354_017_0] showing patches of middle member which overlie blue CBU, with the larger example showing blue-white colors with curvilinear fractures, and smaller, more eroded examples being more yellow in color;

e) HiRISE IRB [ESP_037070_1985] showing a 54 m-tall mound with layered upper member overlying a ~6 m thick orange layer at its base. Inset shows bright-toned meter-scale boulders demarcating the base of layers within the upper member; f) HiRISE IRB [ESP_051905_1990] showing draping meter- to decameter-scale layers (white arrows) in the flank of a pale-toned mound. North is up, unless stated otherwise.

Figure 4: Generalised stratigraphic column of the mound and inter-mound areas showing the temporal relationship between observed morphostratigraphic landing site units, and the mound members (this study), including the inferred hiatuses between them and the interpolated surfaces of Figure 2. This diagram does not show the physical relationships between units and members, and is derived from multiple observations of members and contacts; orange ovals and connectors denote panels in Figures 3 and 5 where the best examples of members and their stratigraphic relationships can be seen.

Figure 5: Mounds in Oxia Planum, showing stratigraphic and tectonic relationships: a) rounded mound on the rim of a ~2 km diameter crater (Sardinia Lacus) in the CBU, which has been later infilled by DRU (HiRISE, ESP_047501_1985); b) 3D 2x exaggerated view of mound showing the mound-CBU boundary (see inlay), which is elevated ~20 m above the topographic mound boundary (HiRISE, PSP_009880_1985); c) mound with upstanding linear features (red) showing a ~60° intersection angle at the mound centre (HiRISE, ESP_048358_1985); d) a mound showing similar features to that in (c), where upstanding linear to curvilinear features truncate a mound at a ~60° intersection angle (HiRISE, ESP_037070_1985); e) intra-crater and crater-rim mound on the rim of Malino Crater, where the CBU has been exposed through the backstepping of DRU and/or mound material (HiRISE, ESP_062191_1985); f) intra-crater mound in Malino Crater, where the onlap of the DRU onto the mound flank (red dashed line) is clearly visible on fractured the lower member or CBU, with an additional DRU layer in yellow (ESP_062191_1985); g) mound with two members: a thin blue-toned middle member (MM) that underlies both the DRU, and an upper member (UM) which is yellow-white (CaSSIS, MY35_007623_019_0); h) orange and blue-toned members of the CBU overlain by mounds; shorter mounds (black arrow) and the bases of tall mounds (red arrow) are white-blue, suggesting the presence of the lower member or

middle member, and upper sections (upper member) are yellow-white (white arrow; CaSSIS, MY35_008742_019_0). North is up, unless stated otherwise.

Number of Mounds	396
Mean Height	18.4 m
Maximum Height	157 m
Mean Area	0.12 km^2
Maximum Area	2.83 km^2
Minimum Elevation at Mound Base	-3176 m
Maximum Elevation at Mound Base	-2771 m
Mean Elevation at Mound Base	-3058 m
Elevation Range	406 m
Mean Aspect Ratio	0.68
Mean Orientation	91.2°

Table 1: Summary Oxia Planum mound morphometric and elevation data.

	Mean Thickness (m)	**Volume (km^3)**
Minimum removed overburden (MUBS – CTX)	41.4	208
Estimate of total removed overburden (CPUBS – CTX)	129	680
Minimum removed mound material (MUBS – LBS)	21.6	124
Estimate of total removed mound material (CPUBS – LBS)	112	605
Material removed below lower mound boundary (LBS – CTX)	19.8	84

Table 2: Summary of eroded thicknesses and volumes of the mound-forming layer in the Oxia Planum study area.

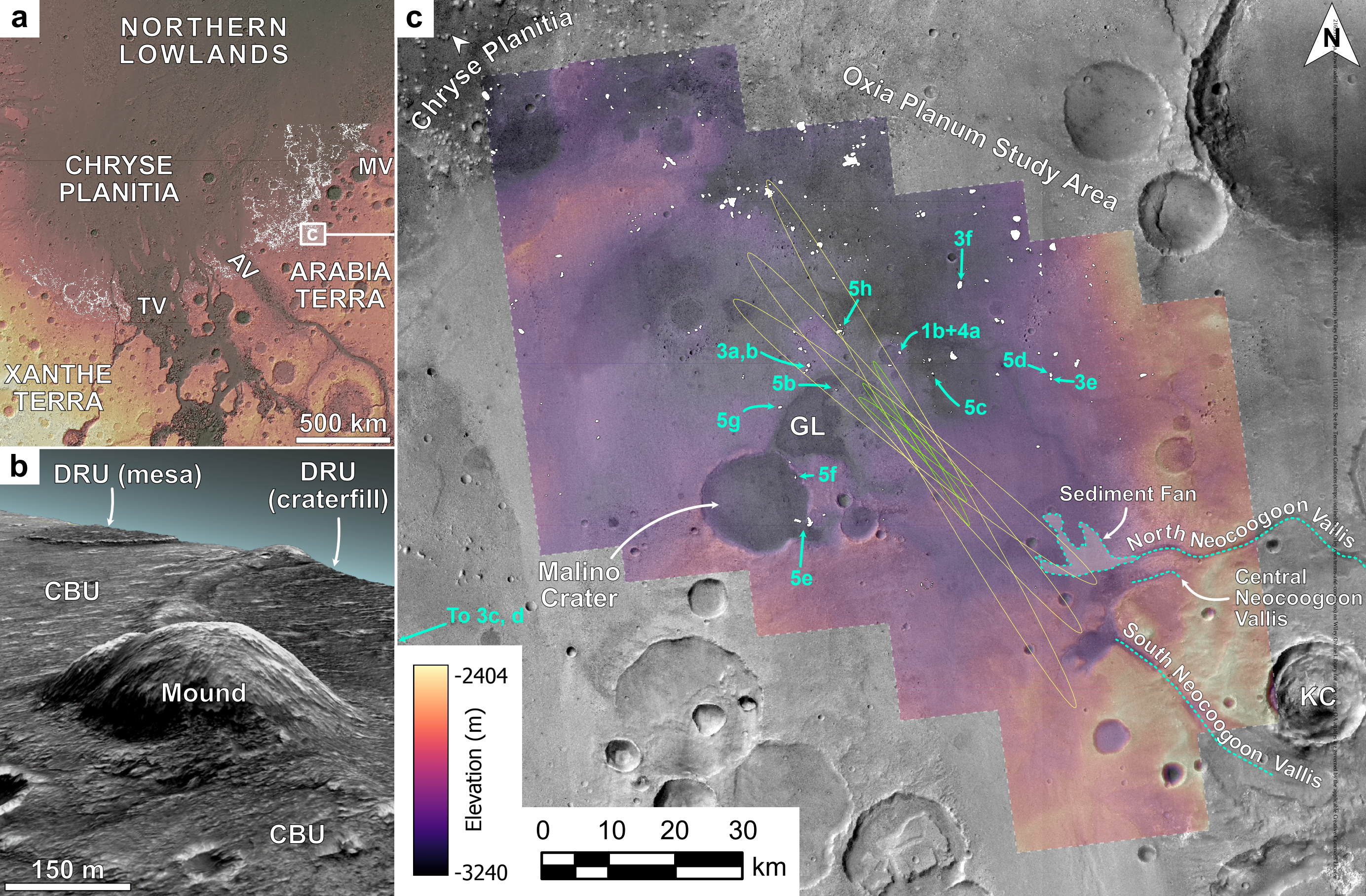
a
NORTHERN LOWLANDS
CHRYSE PLANITIA
MV
c
AV
ARABIA TERRA
TV
XANTHE TERRA
500 km
b
DRU (mesa)
DRU (craterfill)
CBU
Mound
CBU
150 m
c
Chryse Planitia
Oxia Planum Study Area
N
3f
5h
1b+4a
3a,b
5d
3e
5b
5c
5g
GL
5f
Sediment Fan
North Neocoogoon Vallis
Malino Crater
5e
Central Neocoogoon Vallis
To 3c, d
South Neocoogoon Vallis
KC
-2404
Elevation (m)
-3240
0 10 20 30
km

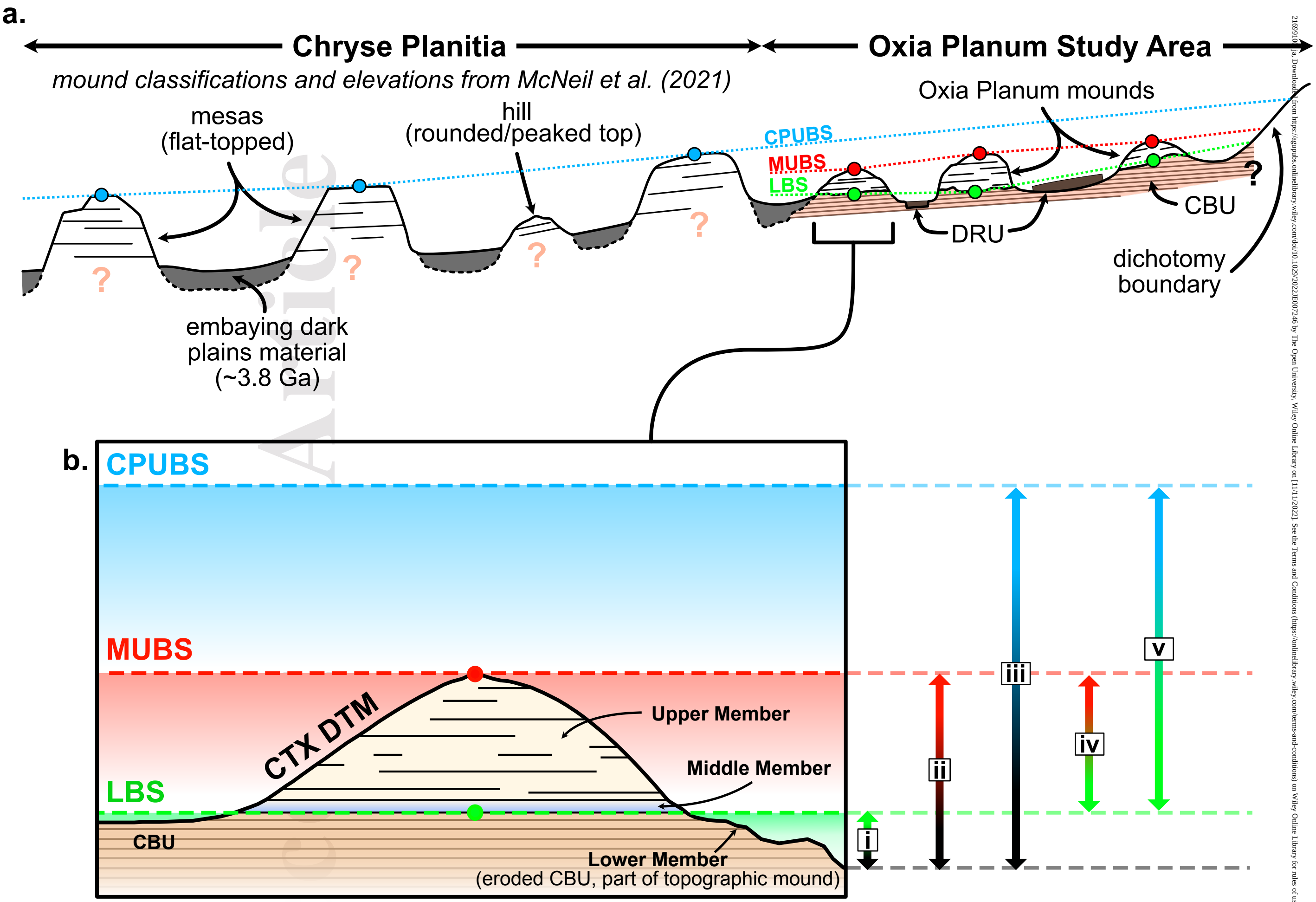

i. LBS - CTX: volume of material removed below LBS (either mound or CBU material)

ii. MUBS - CTX: estimated minimum total amount of material removed

iii. CPUBS - CTX: estimated total volume of material removed

iv. MUBS - LBS: estimated minimum amount of removed mound material

v. CPUBS - LBS: estimated total amount of removed mound material

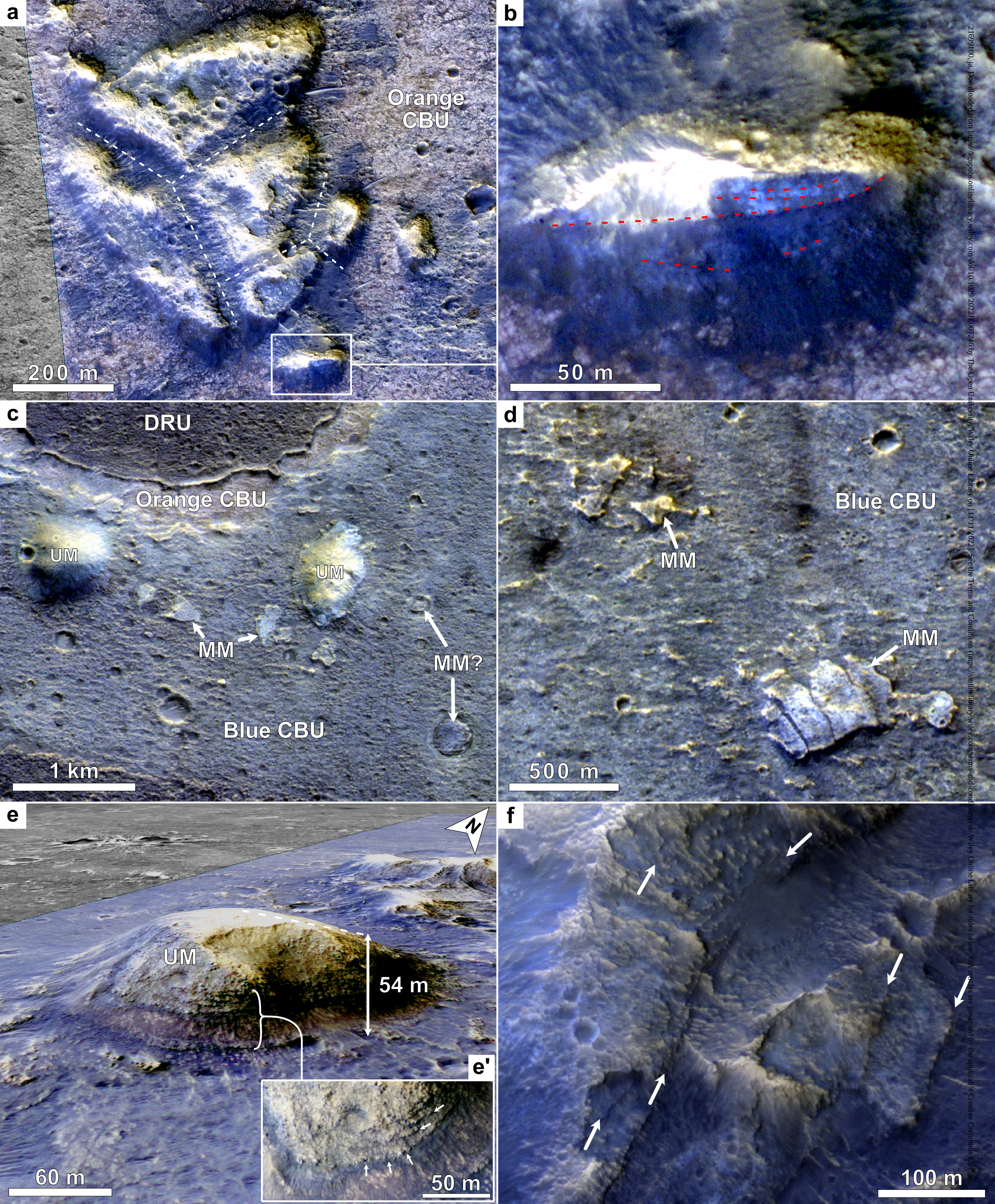
a
Orange CBU
200 m
b
50 m
c
DRU
Orange CBU
UM
UM
MM
MM
MM?
Blue CBU
1 km
d
Blue CBU
MM
MM
500 m
e
N
UM
54 m
e'
50 m
60 m
f
100 m

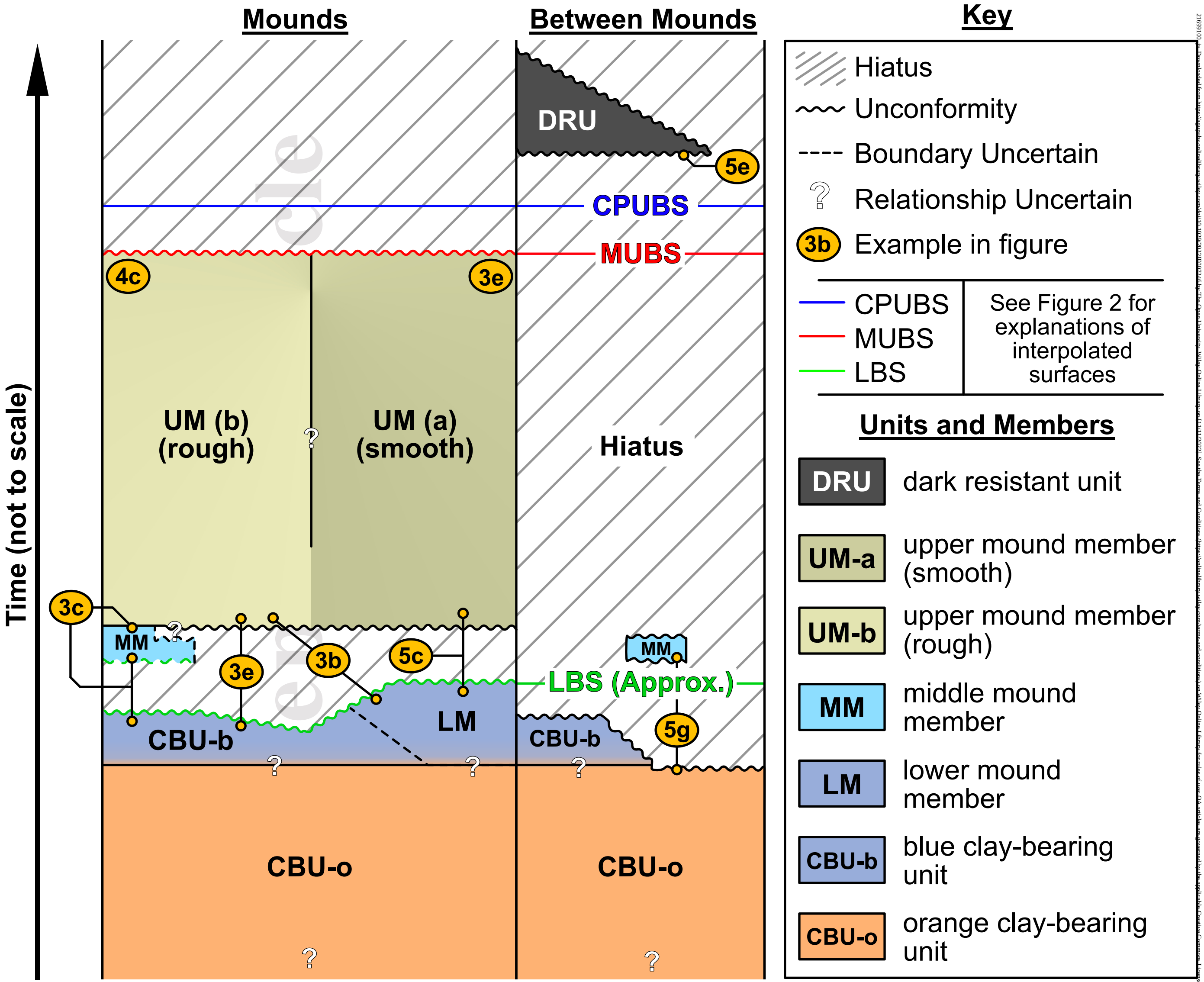
Mounds
Between Mounds
Key
Time (not to scale)
DRU
5e
CPUBS
MUBS
4c
3e
UM (b)
(rough)
UM (a)
(smooth)
Hiatus
3c
MM
3e
3b
5c
LM
MM
LBS (Approx.)
5g
CBU-b
CBU-b
CBU-o
CBU-o
Hiatus
Unconformity
Boundary Uncertain
Relationship Uncertain
3b
Example in figure
CPUBS
MUBS
LBS
See Figure 2 for explanations of interpolated surfaces
Units and Members
DRU
dark resistant unit
UM-a
upper mound member (smooth)
UM-b
upper mound member (rough)
MM
middle mound member
LM
lower mound member
CBU-b
blue clay-bearing unit
CBU-o
orange clay-bearing unit

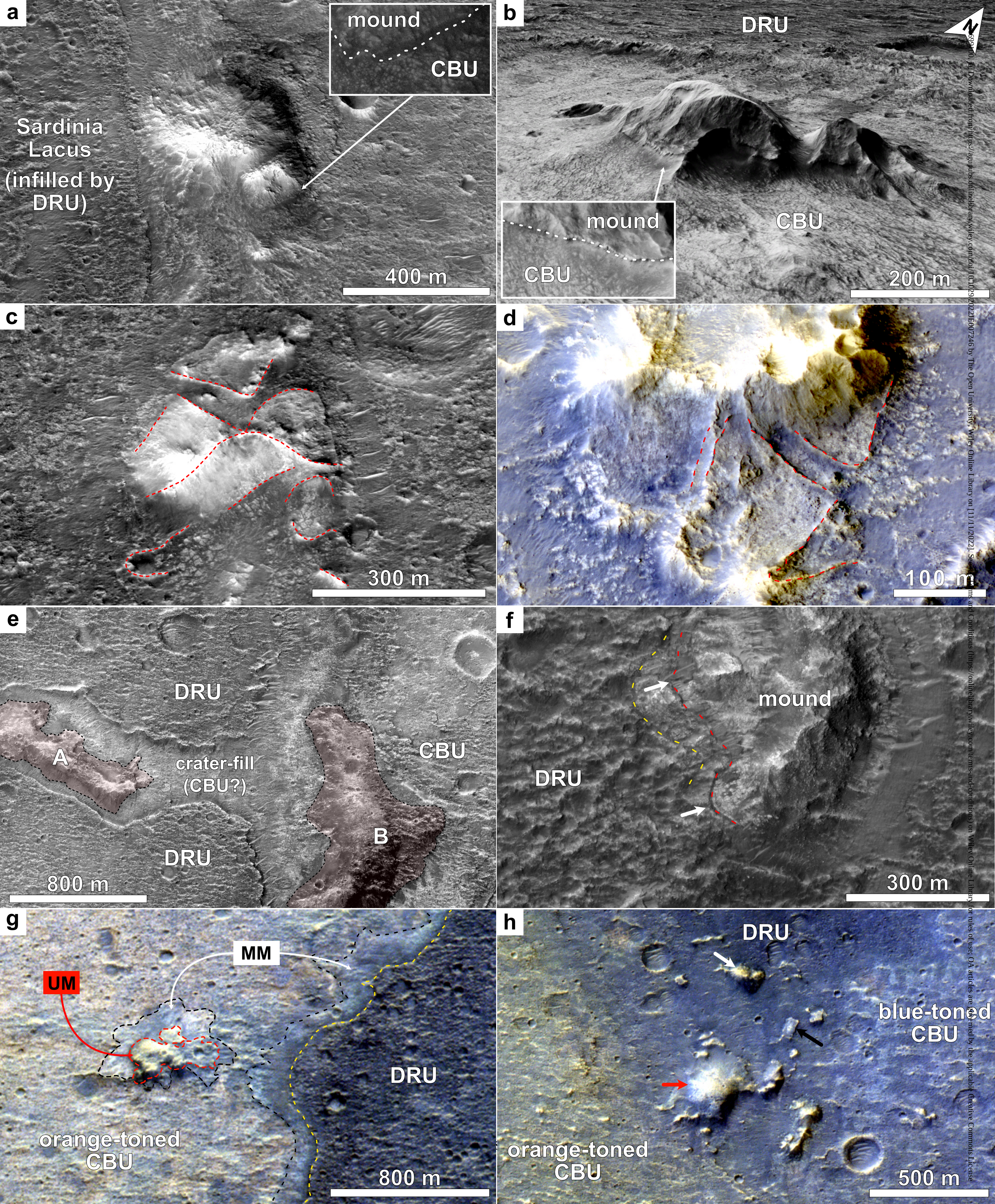

a
mound
CBU
Sardinia Lacus (infilled by DRU)
400 m
b
DRU
N
mound
CBU
CBU
200 m
c
300 m
d
100 m
e
DRU
A
crater-fill (CBU?)
CBU
B
DRU
800 m
f
mound
DRU
300 m
g
MM
UM
DRU
orange-toned CBU
800 m
h
DRU
blue-toned CBU
orange-toned CBU
500 m